# Design of a surgical stapler for laparoscopic colectomy

Dhruva Khanzode[1,2], Ranjan Jha[1,2] Alexandra Thomieres[3], Emilie Duchalais[3], and Damien Chablat[4]

[1] CSIR-Central Scientific Instruments Organisation, Chandigarh-160030, India,
(khanzode.dhruva, ranjan.jha)@csio.res.in,
[2] Academy of Scientific and Innovative Research (AcSIR), Ghaziabad-201002, India
[3] CHU Nantes, Centre hospitalier universitaire de Nantes, France
(alexandra.thomieres,emilie.dassonneville)@chu-nantes.fr,
[4] Nantes Université, École Centrale Nantes, CNRS, LS2N, UMR 6004,
44000 Nantes, France
damien.chablat@cnrs.fr

**Abstract.** In this article, a flexible surgical stapler mechanism is designed to serve as a basis for laparoscopic rectal cancer surgery in which conventional tools cannot be easily accessed. The mechanism is designed by implementing a stacked tensegrity mechanism with a flexible beam as the central spine. The workspace analysis for the stapler was done by studying collaborative data of CT scans of the surgical site from the Axial, Coronal, and Sagittal planes at different intervals. The kinematic equations for the mechanism were synthesized using Hooke's law with a rotational spring and bending moment. For the tensegrity mechanism, singularities and simulations of the mechanism were also analyzed incorporating the eyelet friction parameter. The results of the study signify that the friction parameter can modify the radius of curvature of the mechanism and needs to be analyzed correctly.

**Keywords:** Surgical stapler, anastomosis, laparoscopy, tensegrity mechanism

## 1 Introduction

The field of medical science has grown by leaps and bounds during the last two decades. Minimally invasive surgical procedures have emerged as one of the preferred alternatives for most conventional surgeries. Minimally invasive surgical procedures require very small incisions over the body and specialized slender tools that have miniature tools are inserted through those incisions. These miniature tools have also been modified and modernized over the period of time. Previously, these tools were manually controlled and operated, but nowadays, these tools are being operated using robotic systems. Also, nowadays, robotic systems are also being used in various fields of medical science, like diagnosis, drug delivery, and therapy.

One such procedure is colectomy, wherein all or some part of the colon is removed due to numerous reasons like infection, cell death, tumor, etc. During this procedure, the damaged part of the colon is separated and the rest of the healthy colon tissues or segments are joined together. The joining of the colon segments or any tubular segment is called anastomosis. To perform colon anastomosis, a specialized surgical tool is required known as a "surgical stapler" [1].

The first surgical stapler was invented in 1908 by Victor Fischer and Hümér Hültl. This device was initially developed to prevent the risk of infection due to spillage of Gastro-Intestinal contents on the wounds of patients undergoing abdominal surgeries. The idea was to seal and shut the hollow organs before their division, hence preventing spillage. The surgical stapler was then called a "mechanical stitching device" [2] but later, the design was known as the "Fischer-Hültl stapler". The first modern stapler was invented in 1964 by Mark Ravitch, Leon Hirsch, and Felicien Steichen under the banner of the United States Surgical Corporation (USSC). The USSC products became so popular that their acronyms are still used as a part of surgical vocabulary such as TA, thoracoabdominal, GIA, GI anastomosis. With such success, a competitor named Ethicon appeared in 1997, which was then and still is a subsidiary of the Johnson & Johnson brand and USSC itself successively became Covidien, which is now a part of medical & healthcare giant Medtronics.

In today's surgeries, generally, five kinds of staplers are used, namely TA, Thorasic-Abdominal; GIA, Gastro-Intestinal Anastomosis; Endo GIA, Endoscopic Gastro-Intestinal Anastomosis; EEA, End-End Anastomosis and Skin Stapler. The TA stapler is not equipped with a knife to cut the tissue after the firing of stapler pins and hence the tissue needs to be separated manually. The EEA stapler provides circular staples and the skin stapler is used to close superficial wounds. The TA stapler is most prominently used in veterinary surgical procedures [3]. GIA and Endo GIA are the most used staplers for abdominal surgeries and the Endo GIA staplers are specifically used for minimally invasive surgical procedures [4]. Presently, the Endo GIA staplers are available in 3 forms: passive articulated wrist type (PAW), active articulated wrist type (AAW), and radial reload type staplers (RR). In PAW, the desired bending of the wrist is achieved by pressing the jaw upon the abdominal wall, whereas in AAW, a lever is provided to articulate the wrist into pre-determined bending angles. RR comes with a fixed "U" shape jaw and has been proven to be very useful for pulmonary surgeries [5]. The RR-type stapler is only commercialized by Covidien Inc. The main drawback of the RR type stapler is that it requires a very large incision to enter the body and hence defeats the purpose of "minimally invasive surgery" [6]. Hence there is a dire need for a surgical stapler that can enter through the laparoscopic openings but can work as an RR-type of stapler inside the body.

To solve the positioning and maneuverability issue of an endoscopic surgical stapler[7], this article discusses the design and development of a hyper-redundant flexible surgical stapler for laparoscopic procedures[8]. The envisioned surgical stapler possesses the capability to flexibly orient itself in complex surgical sites. Its flexibility helps achieve the positioning and orientation of the stapler over

the tissue which will seal and bisect the tissue more efficiently as compared to current conventional endoscopic surgical staplers. The envisioned stapler will have four major parts, namely, the upper jaw, lower jaw, stapling cartridge, and wrist. The upper jaw and the lower jaw will encapsulate the stacked tensegrity mechanism which will enable both jaws to bend in the same plane. The bending will be actuated by pushing or pulling of tendons engaged in the tensegrity mechanism [9, 10]. The stapling cartridge will house the surgical staple pins and the cutting knife. The firing mechanism of the cartridge will enable the stapling pins to engage with the tissue as well as actuate the knife to separate the tissue simultaneously. The wrist attached to the base of the jaw will also have a flexible structure able to move in the same plane as the upper and lower jaws. The bending of the wrist will have another couple of tendons for its actuation and the opening and closing of the jaws will be actuated separately. So overall, for the complete operation of the flexible surgical stapler, a total of 4 actuators will be required, (i) for bending of the wrist, (ii) for the firing of staple pins and knife, (iii) for opening and closing of jaws, and (iv) for bending of the upper and lower jaw, which will be actuated synchronously and by a combined single actuation.

## 2 Workspace Analysis

In the field of design and modeling, the first step is to analyze the problem statement provided, followed by determining the limitations and constraints that the design will encounter. Therefore, the first constraint for the design is the available workspace. For viably designing a flexible surgical stapler it is required to investigate how much workspace is available for the stapler to maneuver. Many times, it happens that the total area available is very limited and it is hard to maneuver the surgical tool inside the intended surgical site. Therefore, while developing a new minuscule surgical tool, it is required to analyze the actual space available for the tool move. Typically, computed tomography (CT) scans are used to estimate available space. For our analysis, we collected data for patients who were admitted for colon surgery. The abdominal workspace volume is highly dependent on the age, sex, weight, and physiology of the patient. To illustrate our research, we have the data of a male patient aged 65 years, measuring 1.66 m and weighing 55 kg. This patient was particularly selected as his physiological characteristics provided the smallest workspace volume for the flexible surgical stapler. We proceeded to record the data in the form of CT scans of the generalized surgical site along the three anatomical planes, namely Axial, Coronal, and Sagittal at the interval of 3.33mm for all the planes respectively. The data was then marked by an experienced surgeon for dimensional parameters of the surgical site, represented by red and blue markings in Fig. 1 for each plane respectively using CARESTREAM software. This data was first analyzed to estimate the highest volume of workspace available for the flexible stapler. Second, we can identify the smallest cross-sectional area present at the surgical site. A 3D model is created to simulate stapler placement and laparoscopic insertion.

Thus, we can determine the size of the tool that can be used in this smallest available area.

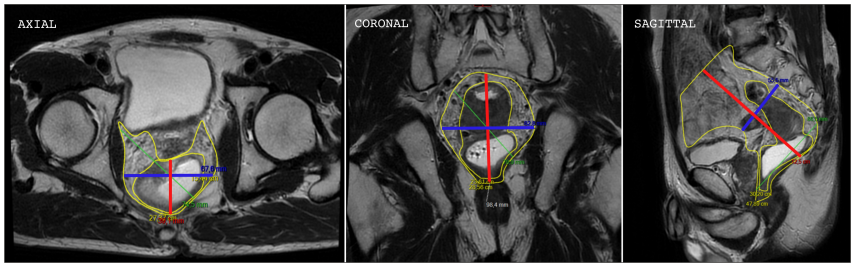


**Fig. 1.** Sample CT scan data for workspace evaluation in Axial, Coronal, and Sagittal planes. The red and blue markings represent the available dimension (mm) in each plane.

## 3 Mechanism design of surgical stapler

For a flexible mechanism, usually, large deflections or deformations are non-linear in nature, therefore, for simplification in kinematic modeling, the constant curvature technique is adopted. Constant curvature mechanisms have a finite number of curved segments. These segments are described by a quantitative set of arc parameters which could be modified into analytical frame transformations. The piece-wise constant curvature approximation (PCCA) presented in the prior art helps us provide the direct kinematics of the mechanism taking the tendon or cable tension as input and giving posture as an output. Sometimes, the flexible mechanism can have a singular flexible spine for all of its segments, but in that case, too, the PCCA can be applied [11]. The constant curvature approximation technique has been successfully applied to various flexible mechanisms, some of which also serve in the medical science and surgery [12].

In this article, the mechanism under study comprises three trapezoidal segments Ⓐ, Ⓑ and Ⓒ, stacked one above the other, as depicted in Fig. 2. This is a new formulation of the tensegrity mechanism defined in [13]. For connecting the base to the mobile platform of each segment, a continuous flexible beam is incorporated capable of deformation in the plane, but with good stiffness in the plane (Fig. 2). The link $A_0J_0$ is a continuous beam from the base to the tip of the mechanism. But, for the sake of analysis, we are taking into consideration only a section of it, i.e. $A_0D_0$, and are analyzing by using the piecewise constant curvature approximation (PCCA). The base platform and the moving platform are attached with the help of two cables/tendons $\rho_1$ and $\rho_2$, present on either side of the central spine and two springs of stiffness $k_1$ and $k_2$ between ($A_1$ $D_1$) and ($A_2$ $D_2$), respectively.

The contraction of the cables will stimulate angular displacement in the flexible beam of the central spine and replication of this phenomenon in each of the three segments will eventually facilitate the bending of the mechanism. The length of the cable is measured as $\rho_i$.

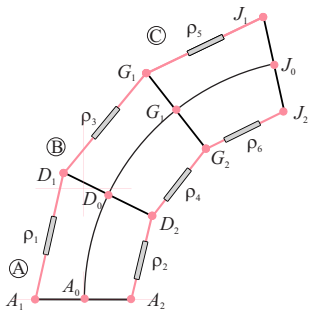


**Fig. 2.** The tensegrity mechanism understudy with three segments stacked, named Ⓐ, Ⓑ, Ⓒ with a flexible beam

### 3.1 Kinematics equations of the tensegrity mechanism

To establish the positions of the points of the mobile platform, it is necessary to study the deformation of a beam subjected to torsion. We assume that the distance between $A_0$ and $D_0$ is $h_1$. The coordinates of the fixed points are:

$$\mathbf{a}_1 = \begin{bmatrix} -l_1 & 0 \end{bmatrix}^T \quad \mathbf{a}_2 = \begin{bmatrix} l_1 & 0 \end{bmatrix}^T \tag{1}$$

To map cable tensions and spring forces for one segment to its radius of curvature, we use a lumped parameter model. For a beam, the springs and cables apply forces on its end that generate a torsional torque:

$$\mathcal{T}_1 = \mathcal{T}_{f1} + \mathcal{T}_{f2} + k_1(\rho_1 - l_{01})l_2 - k_2(\rho_2 - l_{02})l_2 \tag{2}$$

where $\mathcal{T}_{f1} = -f_1 l_2$ and $\mathcal{T}_{f2} = f_1 l_2$. Equation 3 is a Hooke's law with a rotational spring and the bending moment where $K_\theta$ is an effective bending stiffness (in N· m/rad), $h_1$ is the arc length between $A_0$ and $D_0$, $f_1$ and $f_2$ the forces applied by the two cables and $r_1$ is the radius of curvature (See Fig. 3). For one section, we have

$$h_1/r_1 = \mathcal{T}_1/K_\theta \tag{3}$$

Beam characterization may be expressed by its bend radius $r_1$ and the angle $\theta_1$

$$r_1 = h_1/\theta_1 \quad \text{and} \quad \theta_1 = \tau_1/K_\theta \tag{4}$$

This definition stands when we bend in one direction, either left or right and it allows us to perceive the position of $D_0$.

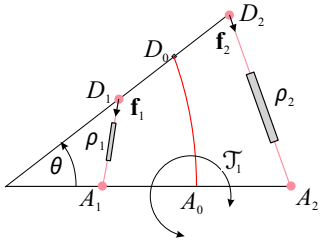


**Fig. 3.** Bending moment equilibrium [12] when two forces $f_1$ and $f_2$ are applied to generate the torque $\mathcal{T}_1$.

The segment $(D_1D_2)$ is normal to the beam at point $D_0$ and the coordinates of these points are

$$d_0 = \begin{bmatrix} r_1 - r_1\cos(\theta_1) \\ r_1\sin(\theta 1) \end{bmatrix} \tag{5}$$

$$d_1 = \begin{bmatrix} r_1 - r_1\cos(\theta 1) - l_2\cos(\theta 1) \\ R\sin(\theta 1) + l_2\sin(\theta 1) \end{bmatrix} \tag{6}$$

$$d_2 = \begin{bmatrix} r_1 - r_1\cos(\theta 1) + l_2\cos(\theta 1) \\ R\sin(\theta 1) - l_2\sin(\theta 1) \end{bmatrix} \tag{7}$$

The inverse kinematic model for a mechanism with a flexible beam is as follows:

$$||\mathbf{a}_1 - \mathbf{d}_1|| = \rho_1, \quad ||\mathbf{a}_2 - \mathbf{d}_2|| = \rho_2 \tag{8}$$

These equations can also be expressed as functions of the lengths of the springs, therefore

$$(-l_1 - r_1 + r_1\cos(\theta 1) - l_2\cos(\theta_1))^2 + (-r_1\sin(\theta_1) + l_2\sin(\theta_1))^2 = \rho_1^2 \tag{9}$$

$$(l_1 - r_1 + r_1\cos(\theta_1) + l_2\cos(\theta_1))^2 + (-r_1\sin(\theta_1) - l_2\sin(\theta_1))^2 = \rho_2^2 \tag{10}$$

Similar to previous assumptions, for sections Ⓑ and Ⓒ, we can write the equations in the same way for the positions of the joints. The inverse kinematic model of the sections is given by

$$||\mathbf{d}_1 - \mathbf{g}_1|| = \rho_3, \quad ||\mathbf{d}_2 - \mathbf{g}_2|| = \rho_4, \quad ||\mathbf{g}_1 - \mathbf{j}_1|| = \rho_5, \quad ||\mathbf{g}_2 - \mathbf{j}_2|| = \rho_6 \tag{11}$$

To know the position of the mobile platform due to the application of force in the tendons or cables, it is necessary for us to calculate the radius of curvature and the angle of inclination that satisfies the kinematic model. The optimization problem is written by using Eq. 8. For each segment, the bending moment and the transfer to the previous one should be evaluated. If $f_2 > f_1$, the beam will bend to the right. The cables go through the thought eyelet where there is friction $\mu$. Figure 4 illustrates the transfer of forces before and after the cable passes through the eyelets of the mobile platform. The study of the stability of the segments by taking into account the friction of the cables in the eyelets

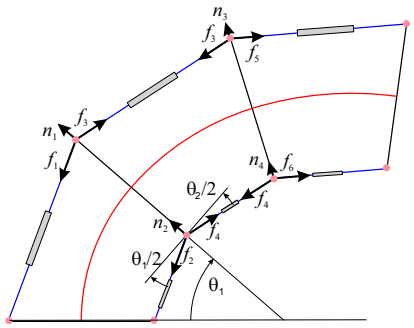


**Fig. 4.** Static equilibrium of three segments

enables the force transmission factors to be obtained [12]. For even values of actuators, the tensions in the cables reduce from the base to the end as

$$\frac{f_{i+3}}{f_{i+1}} = \left(\frac{1-\mu\sin(\theta_1/2)}{1+\mu\sin(\theta_1/2)}\right) \tag{12}$$

For odd values of actuators, the tensions in the cables increase from the base to the end as

$$\frac{f_{i+2}}{f_i} = \left(\frac{1+\mu\sin(\theta_1/2)}{1-\mu\sin(\theta_1/2)}\right) \tag{13}$$

### 3.2 Simulation and singularities

This section promotes a simulation study to show the mechanism's behavior. Some of the model parameters cannot be defined at this time without careful selection of materials and complete knowledge of the workspace within the semicolon. Figure 5 depicts the bending motion when $f_1 - f_2 = 0 + \epsilon$ to 17 N. A slight offset has to fix with $\epsilon$ to avoid the radius of curvature tending to infinity. If we apply the length constraints on the springs having a spring constant of 100 N/m, this movement is not entirely feasible. The extreme position is reached when one of the springs is of zero length (or its minimum length) or when the cable becomes tangent to the bent. By using the constraint into the spring lengths (40% of the spring length in the home pose), the maximal angle is 1.15 rad ($\approx 130°$).

The simulation allows us to solve the inverse kinematics from Eqs. 8, and 11 by using the same optimization algorithm as for a single segment. The simulation of the flexion of the mechanism without friction makes it possible to obtain a perfect curve, without discontinuity between each segment as shown in Fig. 6 (left). The MAPLE software optimization package resolver was used to determine the beam curvature based on cable forces and spring tensions.

When friction is added, the tensions in the two cables are no longer the same in each segment, which changes the curvature as shown in Fig. 6 (right). It is important to note that the model we use is simplified because it assumes that the angle of curvature does not vary from one segment to the next.

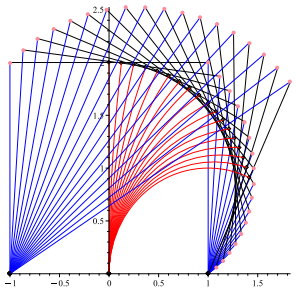

**Fig. 5.** Simulation of the bending of one segment with $l_1 = l_2 = 1$ cm and $h_1 = 2$ cm

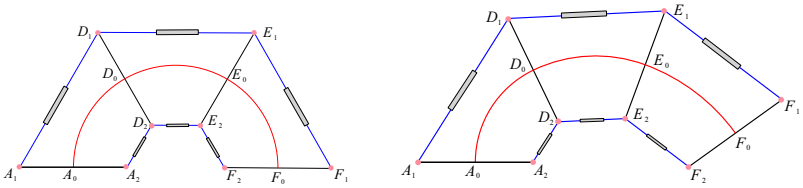


**Fig. 6.** Simulation of bending for three segments with $\mu = 0$ (left) and $\mu = 0.2$ (right) with $l_1 = l_2 = 1$ cm and $h_1 = 2$ cm

## 4 Application to the stapler design

The physical constraints arising due to limited and complex workspace inside the patient's body reduce the cross-section of each segment. Figure 7 illustrates how the designed tensegrity mechanism is positioned in a physical system to create a bendable stapler.

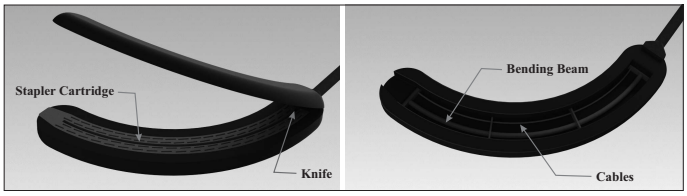


**Fig. 7.** Integration of the mechanism inside the stapler

The problem with this design is that, due to the smaller width of the cross-section, the folding beam reaches the actuating cables even for a smaller angle of deviation, therefore resulting in a greater radius of curvature (Fig. 8). To ensure that the patient's workspace is accessible, another joint must be added similar to a wrist before the stapler. Another solution to this problem is to increase the number of segments, but doing so will result in an increase in the number

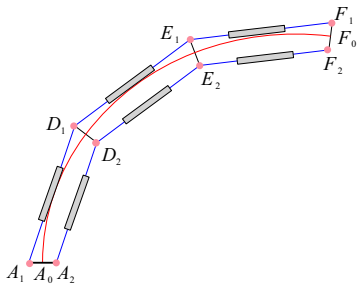


**Fig. 8.** Reduction of the cross-section of the mechanism to be used inside the stapler with $l_1 = l_2 = 1/5$ cm and $h_1 + h_2 + h_3 = 2$ cm

of eyelets through which the cable passes and this might lead to an increase in total friction between the eyelets and the cable.

## 5 Conclusions

In this article, we have studied a flexible mechanism that can be used inside a stapler during laparoscopic colectomy for rectal cancer and other coloanal procedures, where conventional tools cannot be easily accessed. This mechanism consists of a stack of three tensegrity mechanisms made with rigid bodies, linear springs, cables for actuation, and a flexible beam. The size of the stapler depends on a number of criteria that depend on the patient's anatomy and the constraints of laparoscopy. Patient scans are currently being studied to define the workspace where the surgery is performed. Using a lumped parameter model, the analysis was performed with and without the friction parameter within the eyelet of the rigid segment of each segment. It has been demonstrated that the friction parameter can modify the radius of the curvature and needs to be analyzed correctly.

Future research is underway to analyze the impact of friction between the mobile platform eyelets, through which the cable passes, and the cable itself. Evaluation is underway to find the relationship between friction and the curvature of the mechanism. It is estimated that with an increase in the number of sections, the overall friction will increase hence the curvature of the mechanism will not be as expected. The materials used are currently being evaluated to determine the influence of the sheathing covering the mechanism. The skin of the stapler will be made of elastomer to serve as a spring and ensure the sealing to improve its use as medical equipment.

## Acknowledgements

This research is sponsored by the Indian Council of Medical Research, New Delhi, India under the "Senior Research Fellowship" awarded to Mr. Dhruva

Rajesh Khanzode (File no.5/3/8/46/ITR-F/2022) and supported under MoU between CSIR- Central Scientific Instruments Organisation, Chandigarh, India, and Centrale Nantes, France.

## References

1. A. D. Gaidry, L. Tremblay, D. Nakayama, and R. C. Ignacio, "The History of Surgical Staplers: A Combination of Hungarian, Russian, and American Innovation," *The American Surgeon*, vol. 85, pp. 563–566, jun 2019.
2. A. Akopov, D. Y. Artioukh, and T. F. Molnar, "Surgical Staplers: The History of Conception and Adoption," *The Annals of Thoracic Surgery*, vol. 112, pp. 1716–1721, nov 2021.
3. K. M. Tobias, "Surgical Stapling Devices in Veterinary Medicine: A Review," *Veterinary Surgery*, vol. 36, pp. 341–349, jun 2007.
4. P. Schemmer, H. Friess, C. Dervenis, J. Schmidt, J. Weitz, W. Uhl, and M. W. Büchler, "The Use of Endo-GIA Vascular Staplers in Liver Surgery and Their Potential Benefit:A Review," *Digestive Surgery*, vol. 24, no. 4, pp. 300–305, 2007.
5. T. Ema, "The experience of using Endo GIA™ Radial Reload with Tri-Staple™ Technology for various lung surgery," *Journal of Thoracic Disease*, vol. 6, no. 10, pp. 1482–1484, 2014.
6. D. E. Rivadeneira, J. C. Verdeja, and T. Sonoda, "Improved access and visibility during stapling of the ultra-low rectum: a comparative human cadaver study between two curved staplers," *Annals of Surgical Innovation and Research*, vol. 6, p. 11, dec 2012.
7. L. de Calan, B. Gayet, P. Bourlier, and T. Perniceni, "Chirurgie du cancer du rectum par laparotomie et par laparoscopie," *EMC - Chirurgie*, vol. 1, pp. 231–274, jun 2004.
8. G. Ruffo, A. Sartori, S. Crippa, S. Partelli, G. Barugola, A. Manzoni, M. Steinasserer, L. Minelli, and M. Falconi, "Laparoscopic rectal resection for severe endometriosis of the mid and low rectum: Technique and operative results," *Surgical Endoscopy*, vol. 26, no. 4, pp. 1035–1040, 2012.
9. M. Furet, M. Lettl, and P. Wenger, "Kinematic Analysis of Planar Tensegrity 2-X Manipulators," in *International Symposium on Advances in Robot Kinematics*, vol. 8, pp. 153–160, Springer, 2018.
10. P. Wenger and D. Chablat, "Kinetostatic analysis and solution classification of a class of planar tensegrity mechanisms," *Robotica*, vol. 37, pp. 1214–1224, jul 2019.
11. I. A. Gravagne, C. D. Rahn, and I. D. Walker, "Large deflection dynamics and control for planar continuum robots," *IEEE/ASME transactions on mechatronics*, vol. 8, no. 2, pp. 299–307, 2003.
12. T. Kato, I. Okumura, S.-E. Song, A. J. Golby, and N. Hata, "Tendon-driven continuum robot for endoscopic surgery: Preclinical development and validation of a tension propagation model," *IEEE/ASME Transactions on Mechatronics*, vol. 20, no. 5, pp. 2252–2263, 2015.
13. D. Khanzode, R. Jha, D. Chablat, and E. Duchalais, "Stapler design with stacked tensegrity mechanisms for surgical procedures," in *Proceedings of the ASME 2022 International Design Engineering Technical Conferences & Computers and Information in Engineering Conference*, 2022.